

# Immunomodulatory Effects of Adipose Tissue-Derived Stem Cells on Elastin Scaffold Remodeling in Diabetes

James P. Chow<sup>1</sup>, Dan T. Simionescu<sup>2</sup>, Anna L. Carter<sup>1</sup>, Agneta Simionescu<sup>1\*</sup>

<sup>1</sup>Cardiovascular Tissue Engineering and Regenerative Medicine Laboratory, Department of Bioengineering, Clemson University, Clemson, SC, USA

<sup>2</sup>Biocompatibility and Tissue Regeneration Laboratories, Department of Bioengineering, Clemson University, Clemson, SC, USA and Tissue Engineering and Regenerative Medicine Laboratory, Department of Anatomy, University of Medicine and Pharmacy, Targu Mures, Romania

Diabetes is a major risk factor for the progression of vascular disease, contributing to elevated levels of glycooxidation, chronic inflammation and calcification. Tissue engineering emerges as a potential solution for the treatment of vascular diseases however there is a considerable gap in the understanding of how scaffolds and stem cells will perform in patients with diabetes. We hypothesized that adipose tissue-derived stem cells (ASCs) by virtue of their immunosuppressive potential would moderate the diabetes-intensified inflammatory reactions and induce positive construct remodeling. To test this hypothesis, we prepared arterial elastin scaffolds seeded with autologous ASCs and implanted them subdermally in diabetic rats and compared inflammatory markers, macrophage polarization, matrix remodeling, calcification and bone protein expression to control scaffolds implanted with and without cells in nondiabetic rats. ASC-seeded scaffolds exhibited lower levels of CD8+ T-cells and CD68+ pan-macrophages and higher numbers of M2 macrophages, smooth muscle cell-like and fibroblast-like cells. Calcification and osteogenic markers were reduced in ASC-seeded scaffolds implanted in non-diabetic rats but remained unchanged in diabetes, unless the scaffolds were first pre-treated with penta-galloyl glucose (PGG), a known anti-oxidative elastin-binding polyphenol. In conclusion, autologous ASC seeding in elastin scaffolds is effective in combating diabetes-related complications. To prevent calcification, the oxidative milieu needs to be reduced by elastin-binding antioxidants such as PGG.

*Tissue Eng Regen Med* 2016;13(6):701-712

**Key Words:** Streptozotocin-induced diabetes; Arterial scaffolds; Macrophage polarization; Calcification

## INTRODUCTION

Diabetes is a well-known major risk factor for the progression of cardiovascular disease [1-5]. The prevalence of diabetes is globally on the rise, expected to increase from 366 million people in 2011 to 552 million by 2030 [6]. The central mechanism driving vascular complications in diabetes is chronic inflammation. Hyperglycemia and dyslipidemia induce activation of the endothelium and modifications of matrix components, both changes resulting in inflammation. The formation of advanced glycation end products and interactions with their specific cell surface receptors stimulate the formation of reactive oxygen species (ROS), which, together with dysfunctions of mitochondria, contribute to the oxidative stress in diabetes; indeed, super-

oxide generation is believed to accelerate the pathogenesis of cardiovascular diseases in diabetes [7-11]. Furthermore, increased ROS production positively correlates with activation of innate immunity [12] and, subsequently, monocytes and macrophages infiltrate in diabetic aorta [13]. In addition, the pro-inflammatory state of diabetes has been recognized for its pro-calcification potential [14,15]. Elevated levels and faster progression of arterial calcification are consistently reported in populations with diabetes [16]. Vascular calcification can occur in either the intima, caused by atherosclerosis, or the media of the vessel wall, more associated with diabetic conditions [17].

Tissue engineering is rapidly emerging as a potential solution for the treatment of vascular diseases [18,19]; however, there is a considerable gap in the understanding of how tissue engineered vascular products will perform when implanted in patients with diabetes. We have previously reported on the fate of collagen and elastin scaffolds used for cardiovascular tissue engineering after implantation into diabetic rats [20]. Glycation and oxidation products were detected in both scaffolds and these chemical changes were associated with matrix crosslinking and stiff-

**Received:** February 1, 2016

**Revised:** March 2, 2016

**Accepted:** March 4, 2016

**\*Corresponding author:** Agneta Simionescu, Cardiovascular Tissue Engineering and Regenerative Medicine Laboratory, Department of Bioengineering, Clemson University, 501-1 Rhodes Research Center, Clemson, SC 29634, USA. Tel: 864-656-3729, Fax: 865-656-4466, E-mail: agneta@clemson.edu

ening and elevated states of inflammation and calcification. Diabetes-related alterations are clearly not conducive to graft integration and vascular tissue regeneration. To alleviate glycoxylation, we proposed a pre-treatment of the scaffolds with pentagalloyl glucose (PGG), a matrix-binding polyphenol with intrinsic antioxidant properties, which dramatically protected the scaffolds from diabetes-induced adverse reactions after implantation in diabetic rats [20].

Scaffolds, however, are just one key ingredient in the tissue engineering paradigm; in some applications they must be seeded with cells in order to promote new tissue generation and remodeling, leading to construct integration [21,22]. Adipose tissue-derived stem cells (ASCs) have recently been identified as a promising stem cell source due to their immunomodulatory properties, ability to differentiate into various vascular cells and their availability [23–26]. Stem cell immunomodulation, in particular, holds high potential for tissue engineered construct integration by reducing inflammatory cytokine production, suppressing cytotoxic T-cell proliferation, and stimulating the secretion of anti-inflammatory cytokines such as IL-4 and IL-10 [26–29]. Furthermore, ASCs have been shown to regulate macrophage polarization by reduction of classically activated pro-inflammatory M1 macrophage phenotype in favor of the alternatively activated pro healing M2 macrophage phenotype [30–32]. M1 macrophages are responsible for chronic inflammation, secreting abundant amounts of IL-6, TNF- $\alpha$ , as well as toxic reactive oxygen intermediates and nitric oxide, generated by activated iNOS [33,34].

Suppression of chronic inflammation is key for tissue engineered construct survival and integration. However, the ability of ASCs to moderate the aggressive inflammatory environment that diabetes elicits in response to tissue engineered implants has not been explored. Our hypothesis stated that autologous ASCs would temperate the diabetes-related inflammatory reactions and promote tissue remodeling due to their immunomodulatory properties. To test this hypothesis, we collected ASCs from normal and diabetic rats, seeded them in elastin-derived vascular scaffolds and the constructs subcutaneously in normal and diabetic rats. To further protect the scaffolds from oxidation we also treated elastin scaffolds with PGG before cell seeding and implantation.

## MATERIALS AND METHODS

### Materials

Streptozotocin was purchased from Sigma (S0130). The insulin was Humulin N U-100 NPH, Human Insulin of rDNA origin isophane suspension from Lilly (Indianapolis, IN, USA). AlphaTRAK (Gen II) test strip and the AlphaTRAK Blood Glucose

Monitoring System were from Abbott Laboratories, Animal Health (Abbott Park, IL, USA). Collagenase type I was from Sigma (C0130, 125 U/mg) and Dulbecco's modified Eagle's medium (DMEM) from Cellgro-Mediatech, Herndon, VA, fetal bovine serum from Whittaker Bioproducts (Walkersville, MD, USA) and penicillin and streptomycin from Gibco (Rockville, MD, USA). For immunohistochemistry (IHC) we used the following anti-rat antibodies: rabbit anti-laminin (ab11575, Abcam), monoclonal anti-vimentin (V5255, Sigma), mouse anti-CD8 (GTX76218, GeneTex Inc., Irvine, CA, USA), mouse anti-CD68 (ab31630, Abcam), rabbit anti-iNOS (ab15323, Abcam), rabbit anti-CCR7 (CG1678, Cell Applications Inc., San Diego, CA, USA), mouse anti-CD163 (ab111250, Abcam), rabbit anti-osteopontin (ab8448, Abcam), rabbit anti-alkaline phosphatase (ab108337, Abcam), sheep anti-CD34 (AF6518, R&D Systems, Minneapolis, MN, USA), and rabbit anti-alpha-smooth muscle actin (ab5694, Abcam). The VECTASTAIN Elite ABC reagent, R.T.U. (#PK-7100) and the diaminobenzidine tetrahydrochloride (DAB) peroxidase substrate kit (#SK-4100) were purchased from Vector Laboratories (Burlingame, CA, USA). Alizarin Red 1% aqueous staining solution was obtained from Poly Scientific R&D Corp (Bay Shore, NY, USA). All other chemicals were of highest purity available and were obtained from Sigma Aldrich Corporation (Lakewood, NJ, USA). Carboxyfluorescein diacetate-succinimidyl ester (CFDA-SE) cell tracker was purchased from Life Technologies. High-purity PGG was a generous gift from N.V. Ajinomoto OmniChem S.A., Wetteren, Belgium ([www.omnichem.be](http://www.omnichem.be)).

### Arterial elastin scaffold preparation

Scaffolds were prepared following an alkaline extraction protocol described before, with minor modifications [25]. Briefly, fresh porcine carotid arteries (6–8 cm long, 5–6 mm diameter) obtained from Animal Technologies, Inc. (Tyler, TX, USA), were rendered acellular by incubation in 0.1 M NaOH solution at 37°C for 24 h followed by extensive rinsing with deionized water until pH dropped to neutral. Scaffolds were stored in sterile PBS. This treatment removed all cells and most of the collagen, leaving vascular elastin fibers unaltered. Tubular elastin scaffolds, 2–3 cm long and 1 mm thick were cut open longitudinally before implantation.

### PGG treatment

Arterial elastin scaffolds were treated with sterile 0.1% PGG in 50 mM 4-(2-hydroxyethyl)-1-piperazineethanesulfonic acid, pH 5.5, containing 20% isopropanol, overnight at room temperature under agitation and protected from light. Scaffolds were then rinsed in sterile PBS and stored in sterile PBS containing 1% protease inhibitors and 1% Penicillin-Streptomycin at 4°C.

### Rat model of STZ-induced diabetes

Adult male Sprague Dawley rats ( $n=40$ , weight 300–350 g) were rendered diabetic via a single dose of sterile filtered 55 mg/kg streptozotocin (STZ) solution in 0.1 M citrate buffer (pH 5) by tail vein injection (day zero). Control rats ( $n=40$ ) received an equal volume of vehicle (sterile citrate buffer). Starting on day 3, levels of blood glucose in all diabetic rats were determined 3–4 times per week, using AlphaTRAK (Gen II) test strips on the AlphaTRAK Blood Glucose Monitoring System, designed specifically for animals. Glycemia levels were also assayed weekly in the control, non-STZ treated rats. Diabetes was established ( $>400$  mg glucose/dL blood), and diabetic rats were given subcutaneous injections of long-lasting insulin (2–4 U Isophane) every other day to maintain blood glucose level in a desirable range (400–600 mg glucose/dL blood) and prevent development of ketonuria and weight loss. Control rats exhibited mean glycemic levels of  $128\pm 12$  mg glucose/dL blood. Glucose levels, individual weights, hydration status, and food and water consumption were monitored closely to ensure adequate health parameters. Animals were provided with food and water ad libitum and were cared for by the attending university veterinarian and associated staff at the Godley-Snell Research Center animal facility at Clemson University. The Animal Research Committee at Clemson University approved the animal protocol (AUP 2011-002), and National Institute of Health (NIH) guidelines for the care and use of laboratory animals (NIH publication #86-23 Rev. 1996) were observed throughout the experiment. A detailed time-line of the entire experimental setup including cell collection, seeding, implantation, explantation and a lineup of implant groups is outlined in Figure 1.

### Adipose stem cell isolation and injection into scaffolds

Two weeks after STZ administration, a small amount of subcutaneous abdominal adipose tissue ( $\sim 30$  mg wet) was harvested from each rat via lipectomy under general anesthesia and immediately processed according to the Zuk et al. [35]. Briefly, adipose tissue was minced with blades and incubated with 2 mg/mL collagenase. After centrifugation, cell pellets were treated with 0.155 M ammonium chloride ( $\text{NH}_4\text{Cl}$ ) to lyse red blood cells, and the stromal vascular fraction pellet was plated in tissue culture flasks. Adherent cells were cultured for two weeks in DMEM/10% FBS to propagate the ASCs and then seeded into each elastin scaffold at approximately  $1\times 10^6$  cells per scaffold ( $\sim 5\times 10^4$  cells per  $\text{cm}^2$ ), via injections at multiple sites along the scaffold using a 30 G needle. Each batch of ASC-seeded scaffolds was labeled and cultured separately to allow for implantation of cells into same animal from which the adipose tissue was originally collected (autologous). Cell-seeded scaffolds and scaffolds without cells were incubated overnight in cell culture media in a

standard cell culture incubator at  $37^\circ\text{C}$  and 5%  $\text{CO}_2$  before implantation. For tracking purposes, cells isolated from two animals from each group were labeled before seeding with  $10\ \mu\text{M}$  CFDA-SE, a fixable-cell-permeant, fluorescein-based tracer. IVIS (PerkinElmer, Waltham, MA, USA) was used to image CFDA-SE tagged cells at 2 weeks and 4 weeks after implantation.

### Experimental implant groups

The arterial elastin scaffolds were divided into four groups (Fig. 1) as follows: 1) non-PGG treated scaffolds with no ASCs, 2) non-PGG treated scaffolds with injected ASCs, 3) PGG-treated scaffolds with no ASCs, 4) PGG-treated scaffolds with injected ASCs. Scaffolds were implanted subdermally into control and diabetic rats as detailed below.

### Subdermal implantation of elastin scaffolds

Four weeks after STZ administration (two weeks after ASC isolation), rats were shaved and prepped for surgery and anesthetized using 1–2% isoflurane. Diabetic rats were given 1 U of insulin pre-operatively. A small, transverse incision was made on the back of the rats, and two subdermal pouches were created by blunt dissection. One scaffold was then inserted into each pouch ( $n=2$  scaffolds per rat) and incisions closed with surgical staples. A total of 160 scaffolds have been implanted in 80 rats, of which 40 were diabetic and 40 controls (Fig. 1). Each group of scaffolds described above consisted of 20 scaffolds implanted in 10 rats. The rats were allowed to recover, provided with food and water ad libitum, and were cared for by the attending veterinarian and associated staff at the Godley-Snell Research Center animal facility. Glucose monitoring and insulin treatment were continued for the diabetic rats as described above. Four weeks after scaffold implantation, the rats were humanely euthanized by  $\text{CO}_2$  asphyxiation and the scaffolds explanted and prepared for analysis.

### Histology and immunohistochemistry

Paraffin-embedded scaffolds sections ( $5\ \mu\text{m}$ ) were rehydrated and stained with hematoxylin and eosin (H&E) for a general overview of scaffold integrity and presence of cells.

For IHC, heat-mediated antigen retrieval was implemented by immersing sections in 10 mM citrate buffer (pH 6.0) for 20 minutes at  $95\text{--}100^\circ\text{C}$ . Sections were then treated with 0.025% Triton X-100 for 10 minutes and blocked in 1.5% normal horse serum for 30 minutes. Endogenous peroxidases were blocked with 0.3% hydrogen peroxide in 0.3% horse normal serum for 30 minutes then primary antibody was applied for 1 hour at room temperature. We used the following antibody dilutions and concentrations for IHC: CD34 (1:200), CD68 (1:100), iNOS (1:100), CD163 (4  $\mu\text{g}/\text{mL}$ ), CD8 (4  $\mu\text{g}/\text{m}$ ), vimentin (1:250),

$\alpha$ -smooth muscle actin (1:200) and laminin (1:25). After rinsing, sections were incubated in species-appropriate biotinylated secondary antibody (1:200 dilution, Vector Labs, Burlingame, CA, USA) for 30 minutes. VECTASTAIN Elite ABC Reagent, R.T.U. was applied, and the chromogen was visualized using the DAB Peroxidase Substrate Kit. Negative staining controls were obtained by the omission of the primary antibody. Sections were lightly counterstained with Hematoxylin prior to mounting. Digital images were obtained at various magnifications (25X to 200X) on a Zeiss Axiovert 40CFL microscope using AxioVision Release 4.6.3 digital imaging software (Carl Zeiss MicroImaging, Inc., Thornwood, NY, USA). Relative quantification for IHC stains was performed on ImageJ (provided by NIH) using the ImmunoRatio plugin (ver. 1.0 c) on  $n=3$  sections per group. Quantities are expressed as percentage of DAB area to nuclear area or ECM area, depending on stain type (cellular stain or matrix stain). Each image was adjusted individually for brown threshold and blue threshold to fine-tune each component, as recommended by the software developer [36].

### Calcium and bone protein analysis

Alizarin Red staining for calcium deposits was performed on sections of explanted elastin scaffolds ( $n=5$  per group). Osteopontin (OPN) (1:250 dilution) and alkaline phosphatase (1:300 dilution), were also analyzed in arterial elastin scaffolds via IHC.

### Statistical analysis

Results are expressed as means  $\pm$  standard deviation. Statistical analysis was performed using one-way ANOVA for each marker. Differences between means were determined using the least significant difference with an alpha value of 0.05.

## RESULTS

### *In vitro* and *in vivo* imaging of ASCs seeded into scaffolds

Before implantation, the presence of cells and their distribution in the scaffolds was confirmed by H&E staining (Fig. 2). The presence of ASCs in the scaffolds two weeks after implantation was also confirmed by imaging the CFDA tagged cells via IVIS (Fig. 2). After four weeks, however, the fluorescence of the tagged ASCs could no longer be detected (not shown).

### Impact of ASCs on inflammatory cell infiltration

In order to evaluate the effect of implanted autologous ASCs on the host immune reaction, arterial elastin scaffolds with and without ASCs were implanted in diabetic and non-diabetic rats. After four weeks, scaffolds were explanted and the infiltrated inflammatory cell types were analyzed by histology. Elevated levels

of CD8<sup>+</sup> T-cells (29.3%) and CD68<sup>+</sup> pan-macrophages (14.2%) were noticed to infiltrate the scaffolds implanted in the diabetic rats compared to the non-diabetic rats (13.5% CD8<sup>+</sup> and 1.9% CD68<sup>+</sup>, Fig. 3). However, scaffolds seeded with autologous ASCs exhibited reduced accumulation of both T-cells (10.2%) and pan-macrophages (5.0%) in cell-seeded versus non-seeded scaffolds implanted in diabetic conditions (Fig. 3).

### ASCs effects on macrophage polarization

To assess the number of M1 and M2 macrophages present in implants, sections were stained for iNOS, a marker for M1 macrophages, and CD163, a marker for M2 macrophages. M1 macrophages were seen in large numbers in scaffolds implanted in diabetic rats (20.8%) (Fig. 4) compared to scaffolds implanted in control, non-diabetic rats (6.2%, Fig. 4). In ASC-seeded scaffold

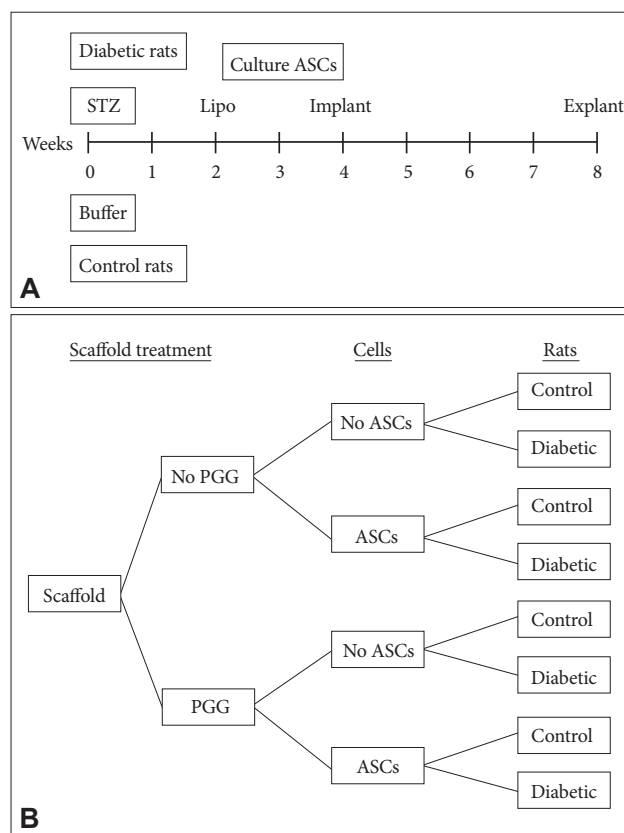


**Figure 1.** Experimental time line and implant groups. (A) Studies started with diabetes induction at “day zero” in 40 rats by a single i.v. injection of streptozotocin (STZ) in citrate buffer. Control rats ( $n=40$ ) received citrate buffer alone. Adipose tissue collection (Lipo) was performed 2 weeks after diabetes induction, which was followed by isolation and propagation of ASCs from each individual rat (2 weeks). Scaffolds were then seeded with autologous ASCs 1 day before subdermal implantation in diabetic or control rats. (B) Overview of implant groups consisting of non-treated scaffolds and scaffolds treated with PGG, seeded or not seeded with ASCs, implanted in control or diabetic rats. ASCs: adipose tissue-derived stem cells, PGG: penta-galloyl glucose.

folds, however, iNOS expression was significantly lowered, only 2.1% in control and 3.3% in diabetic rats (Fig. 4). The opposite trend was seen in the expression of CD163 (M2 macrophages) as there were few CD163<sup>+</sup> cells (0.2%) detected in arterial elastin scaffolds implanted in either diabetic or control rats (Fig. 4). Conversely, an increased number of CD163<sup>+</sup> cells were observed in elastin scaffolds injected with ASCs before implantation; 20.2% in control and 20.0% in diabetic rats (Fig. 4).

### Non-inflammatory cell infiltration and matrix remodeling

In order to evaluate whether cells involved in tissue remodeling were present, we used IHC to detect the type of non-inflammatory cells infiltrated in the implant. Cells positive for  $\alpha$ -smooth muscle actin and vimentin, possible fibroblasts or myofibroblasts, as well as CD34<sup>+</sup> stem cells (Fig. 5) were detected in the adventitia of vascular scaffolds. ASC-seeded scaffolds exhibited greater expression of CD34 (28% increase in control and 41.6% increase in diabetic rats) and  $\alpha$ -smooth muscle actin (14.1% in-

crease in control and 12.7% increase in diabetic rats). Vimentin expression in either scaffold group remained relatively unchanged regardless of glycemic status. Throughout the ASC-seeded arterial elastin scaffolds, we also detected the presence of laminin, a basal lamina protein that provides substrates for cell attachment and migration. Scaffolds without seeded ASC exhibited no endogenous laminin (Fig. 5).

### Calcification and osteogenic responses

Alizarin red staining indicated presence of calcium accumulation in elastin scaffolds without ASCs, regardless of glycemic conditions (Fig. 6A). IHC revealed presence of both OPN and ALP in scaffolds without ASCs implanted in control rats (Fig. 6B). OPN and ALP levels were even more abundant in scaffolds implanted in diabetic rats. Remarkably, no visible calcium or traces of OPN and ALP were observed in the ASC-seeded scaffolds implanted in control rats (Fig. 6A and B). Contrastingly, a significant amount of calcium and high levels of OPN and ALP were observed in the ASC-seeded scaffolds implanted in diabet-

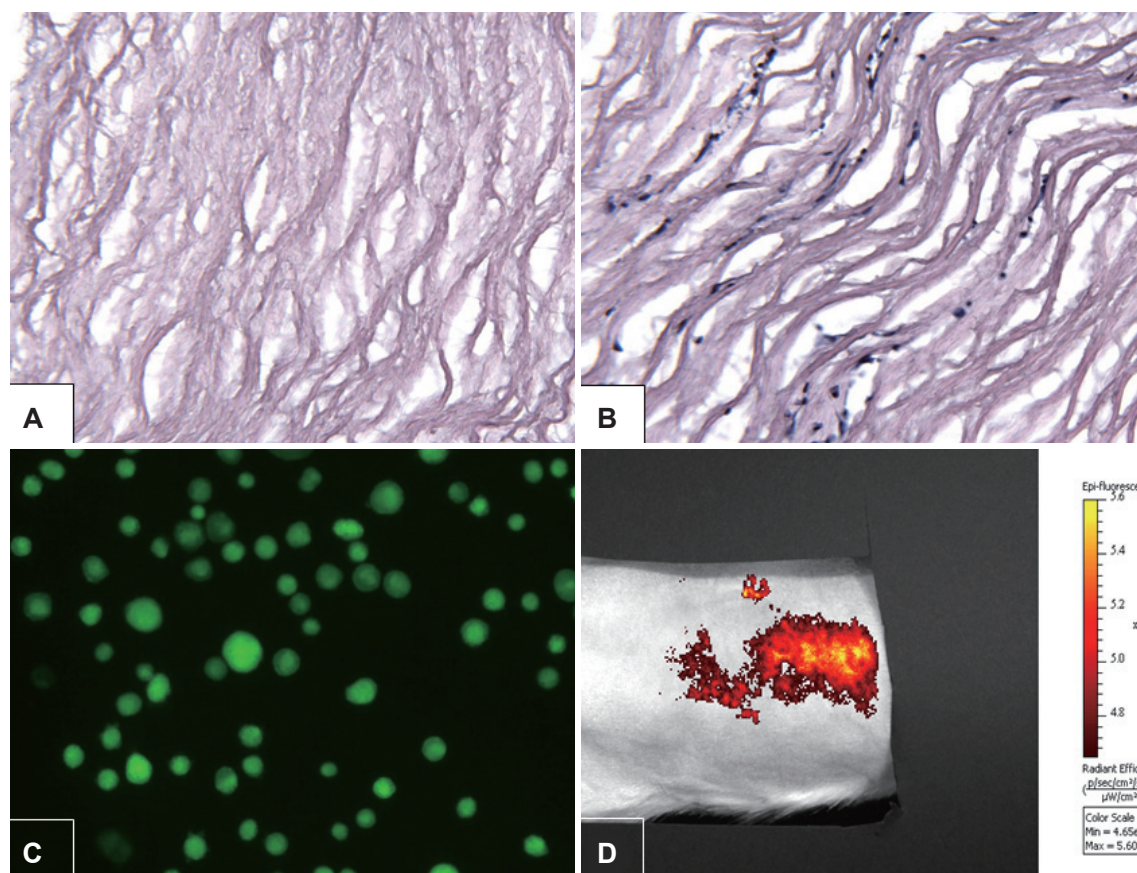


**Figure 2.** ASCs seeding and tracking. Representative histological images of (A) decellularized arterial elastin scaffolds and (B) ASC-seeded elastin scaffolds stained with H&E. (C) Fluorescently tagged ASCs prior to seeding within elastin scaffolds, imaged immediately after trypsinization and tagging with CFDA-SE. (D) Representative IVIS image showing fluorescence of CFDA-SE tagged cells seeded within scaffolds, 2 weeks after subcutaneous implantation. Magnifications are 10 $\times$  for (A), (B), (C), and 1 $\times$  for (D). ASCs: adipose tissue-derived stem cells, H&E: hematoxylin and eosin, CFDA-SE: carboxyfluorescein diacetate-succinimidyl ester.

ic rats. In scaffolds pre-treated with PGG, no visible traces of calcium deposits were noted, regardless of glycemic condition or cell seeding status (Fig. 6A).

**DISCUSSION**

In diabetes, excessive inflammation and oxidation can result in vascular calcification. Tissue engineered vascular scaffolds injected with adipose stem cells can be tested in diabetic animal models. In our studies, we implanted arterial elastin scaffolds

seeded with autologous ASCs subdermally in diabetic rats and compared them to scaffolds without cells, as well as to implants in non-diabetic rats.

We noticed an excessive inflammatory response to the arterial elastin scaffolds implanted in diabetic rats when compared to control rats (Fig. 3). These cells included T-cells and cells staining for pan macrophage markers, but none of these cells were M2 macrophages (Fig. 3 and 4). Consequently, we hypothesized that tissue engineered elastin-based vascular scaffolds implanted in diabetic conditions might undergo impaired remodeling and

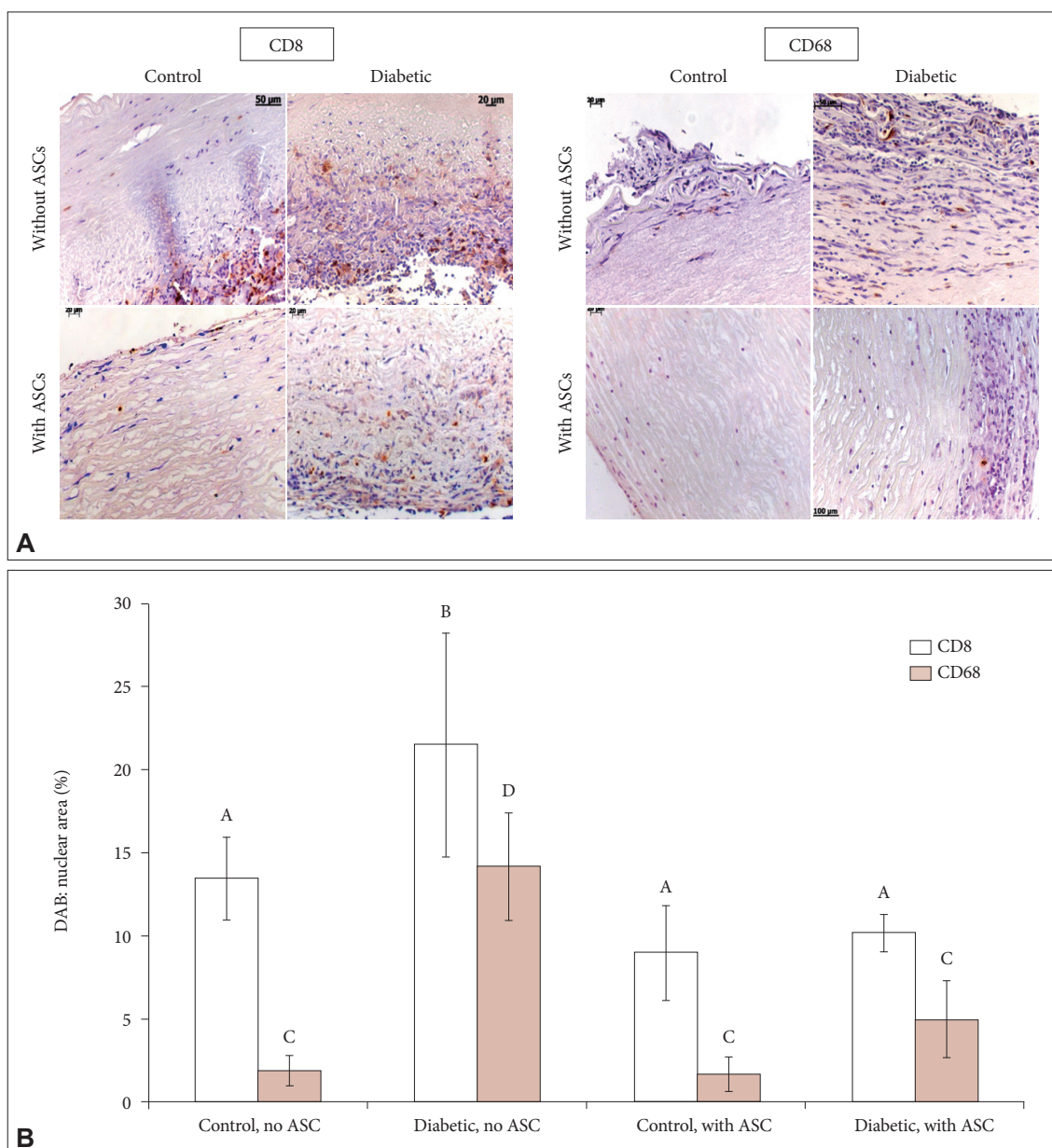


**Figure 3.** Inflammatory cell infiltration. Representative immunohistochemistry images (A) and their quantification (B) of T-cells (CD8) and macrophages (CD68) infiltration in scaffolds with and without seeded ASCs, implanted in control or diabetic rats. Brown=positive. In (B) for each marker, different letters indicate statistical significance ( $p < 0.05$ ) between the four implant groups. ASC: adipose tissue-derived stem cell.

healing, due to chronic inflammation. It has been demonstrated that the host innate immune system responds to implanted biomaterials by recruiting macrophages that amplify the inflammatory response and subsequently send signals to T-cells. However, the ECM-based scaffolds have been shown to promote a switch in the macrophage population from a predominantly pro-inflammatory M1 phenotype to predominantly reparative M2 macrophages, which secrete anti-inflammatory mediators [37,38]. We noticed these effects in scaffolds implanted in control rats, but not in diabetic rats. These observations are in agreement with

studies that show that in diabetes, the combination of persistent hyperglycemia and oxidative stress associated with decreased activity of endogenous antioxidants, lead to chronic inflammation, delayed or impaired wound healing and reduced ability to transition from a M1 to a M2 phenotype macrophages [7,9,39].

Since ASCs are considered a promising stem cell source in tissue engineering, due to their immunomodulatory properties, ability to differentiate into various vascular cells and their availability [23-26], we used autologous ASCs to repopulate the scaffolds. Our goal was to investigate the effect of ASCs on the pop-

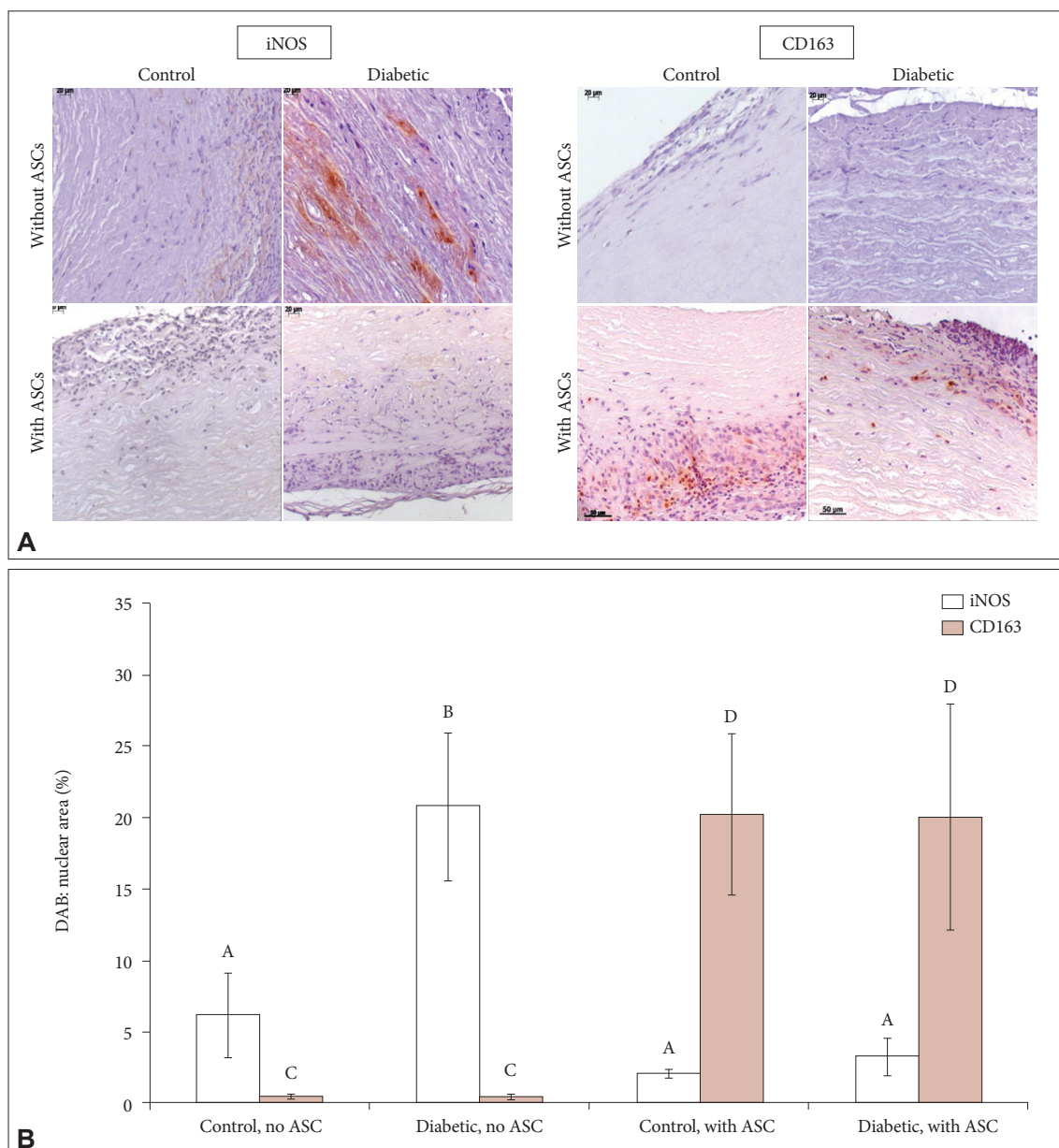


**Figure 4.** Macrophage polarization. Representative immunohistochemistry images (A) and quantification (B) of M1 macrophages, positive for inducible nitric oxide synthase (iNOS) and M2 macrophages positive for CD163, in scaffolds with and without ASCs implanted in control or diabetic rats. Brown=positive. In (B) for each marker, different letters indicate statistical significance ( $p < 0.05$ ) between the four implant groups. ASC: adipose tissue-derived stem cell.

ulation of infiltrated cells, as well as on scaffold remodeling under diabetic conditions. Indeed, as indicated in Figures 2 and 3, the scaffolds injected with ASCs exhibited only 10.2% T-cells and

5% macrophages. Also an increase in M2 cell number was noticed, to 20% in both control and diabetic conditions. The levels of PGE2 measured in explants showed an increase in scaffolds

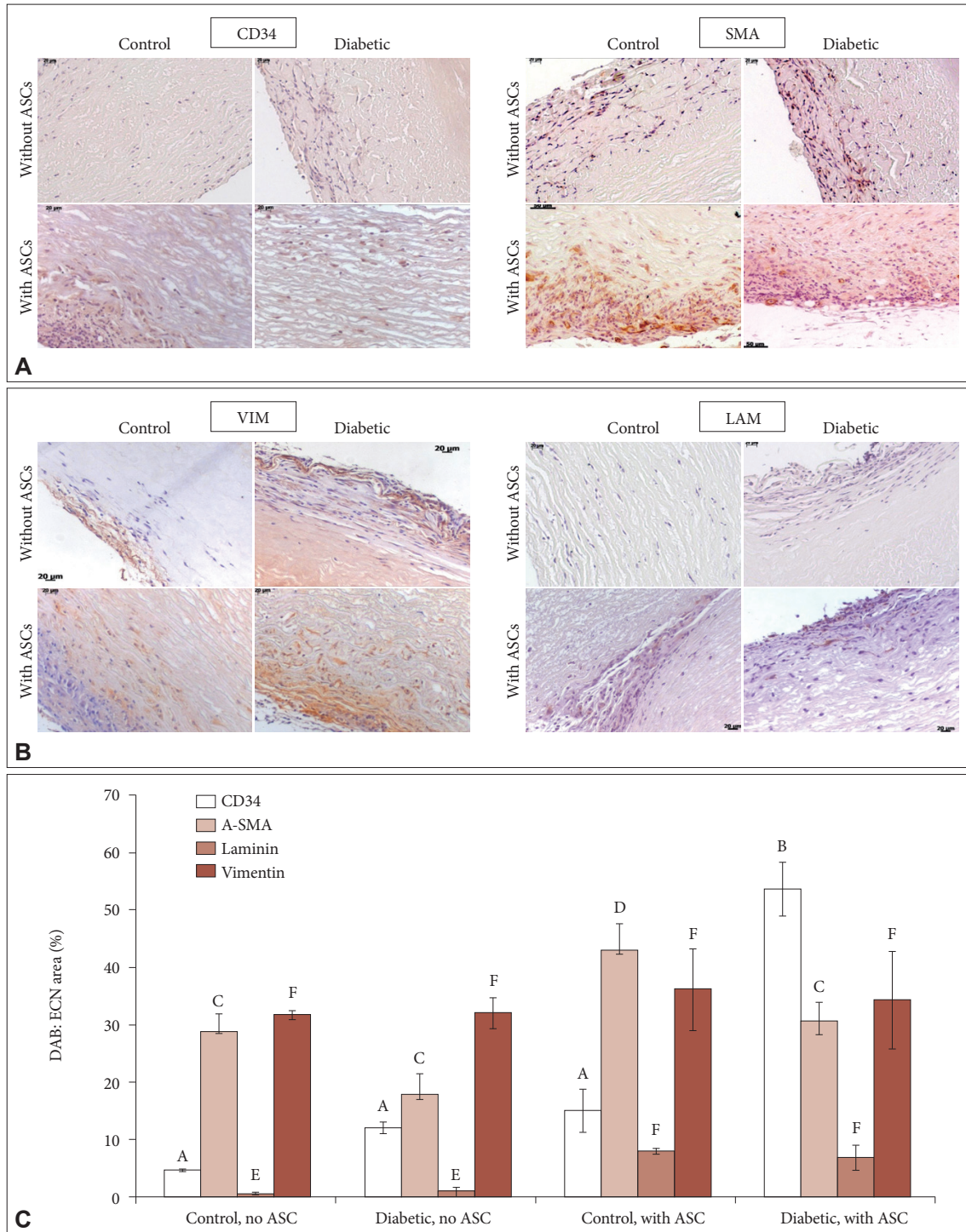


**Figure 5.** Non-inflammatory cell infiltration and de novo synthesis of basement membrane proteins. (A) Representative immunohistochemistry of stem cells (CD34) and myofibroblasts staining for  $\alpha$ -smooth muscle actin (SMA) in scaffolds with and without ASCs implanted in control or diabetic rats. (B) Immunohistochemistry for vimentin (VIM) and laminin (LAM) in scaffolds with and without ASCs implanted in control and diabetic rats. Brown=positive. (C) Quantification of images in (A) and (B). In (C) for each marker, different letters indicate statistical significance ( $p < 0.05$ ) between the four implant groups. ASC: adipose tissue-derived stem cell.



seeded with ASCs (10 pg/mg protein vs. 20 pg/mg protein, respectively). Our results are in agreement with previous papers which showed that ASCs have immunomodulatory properties

and are able to down regulate Th1 cytokines and improve overall Th1/Th2 balance [40] by stimulating production of anti-inflammatory cytokines such as IL-4 and IL-10 [28]. It has been

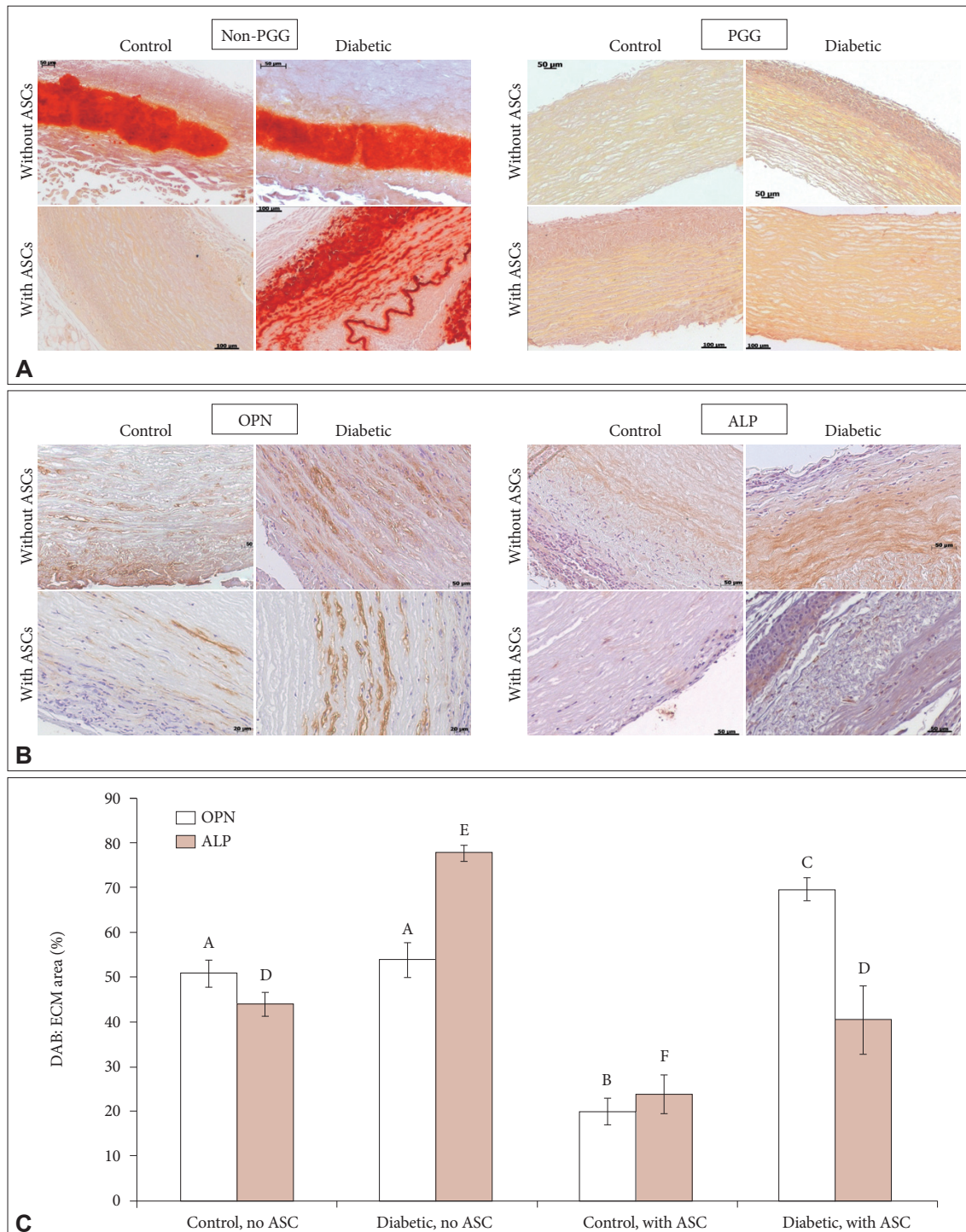


**Figure 6.** Calcification and bone protein expression. (A) Alizarin Red histological stain for calcium deposits (red) in non-PGG treated and PGG-treated arterial elastin scaffolds with and without ASCs implanted in control or diabetic rats. (B) Representative immunohistochemistry for osteopontin (OPN) and alkaline phosphatase (ALP) in scaffolds with and without ASC seeding, implanted in control or diabetic rats. (C) Quantification of images in (B). Brown=positive. In (C) for each marker, different letters indicate statistical significance ( $p < 0.05$ ) between the four implant groups. PGG: penta-galloyl glucose, ASC: adipose tissue-derived stem cell.

demonstrated that ASCs act through paracrine release of growth factors that accelerate and direct tissue repair by host-derived cells [41-43] and secrete prostaglandin to suppress inflammatory responses following ischemic events, thus enhancing recovery [44].

The mechanism by which matrix-based scaffolds promote the transition from M1 to M2 remained unknown, but it has been suggested the role of specific peptide sequences present in the structure of matrix components in the interaction with particular cells [37]. It's been known that specific amino acid sequences in the structure of matrix proteins or their degradation products (i.e., matrikines) may exhibit biological activities, such as chemotaxis, MMP release, and modulation of cell phenotypes, via a 67-kD elastin laminin receptor present on the surface of fibroblasts, smooth muscle cells, and monocytes [45-47]. Together, these matrix peptides and the cytokines secreted by stem cells might encourage a constructive tissue remodeling by attracting not only inflammatory cells, but also cells with tissue regeneration capabilities. In our studies, we noticed the presence of alpha-smooth muscle actin and vimentin positive cells, which indicate fibroblasts or myofibroblasts, cells known to be involved in tissue remodeling (Fig. 5). Indeed, after the implantation of constructs, we detected the presence of laminin, (Fig. 5B), a basement membrane protein fundamental for cell adhesion [19,48,49], differentiation, and maturation [50,51]. These results suggest that the injected and/or infiltrated cells rebuilt their own basement membrane in order to adhere and remodel the scaffolds. Positive IHC staining for CD34 implied the presence of remnant or possibly newly infiltrated stem cells in the elastin scaffolds [25,31].

Vascular calcification is a known occurrence in diabetes and is typically associated with chronic inflammation and oxidative stress. Its mechanism is still not fully understood, but the extracellular matrix calcification in the media has been long noted in animal models of diabetes and dyslipidemia as well as in patients with diabetes type 1 and type 2 [52,53]. Many groups reported similarities to the process seen during end stage renal disease [20,54-59]. Furthermore, osteogenic transformation of graft smooth muscle cells was shown to occur alongside up-regulated pro-inflammatory response caused by TNF- $\alpha$  [60], elastin degradation, and TGF- $\beta$  [61,62]. Hyperglycemia, excessive insulin, and hypoxia can lead to increased bone-like protein expression in smooth muscle cells [53,63,64]. OPN, a protein involved in bone remodeling and osteoclast activation [65], has been shown to be upregulated at inflammatory sites caused by biomaterial implants [66].

We have previously reported on the *in vivo* calcification of elastin scaffolds in both non-diabetic and diabetic conditions [20]. In current experiments, calcium deposits and osteogenic

markers were present in all subdermally implanted scaffolds, except those which had been pre-seeded with ASCs and implanted in control rats (Fig. 6). We believe that this is the first report on the effect of ASCs on calcium accumulation in implanted vascular graft scaffolds. Our data also showed that OPN accumulates in subdermally implanted elastin scaffolds (not seeded with cells before implantation), suggesting a tendency of the infiltrated cells to combat calcification.

However, the ASCs appeared to have had little effect on calcium accumulation in tissues implanted in diabetic rats (Fig. 6A). In diabetes, besides the excessive inflammatory milieu, there is also an increased oxidative environment, well-illustrated by the activation of AGE receptors, which stimulates an overproduction of ROS [67]. For this reason, we treated our scaffolds with an anti-oxidative agent, PGG, before cell seeding. These tissues implanted in diabetic rats showed no calcium accumulation in all samples analyzed (Fig. 6A). PGG is an anti-oxidative polyphenol, which binds to collagen and elastin and protects the fibers from fast degradation and calcification [68]. Many publications have showed that stimulation of AGE receptors result in NADPH oxidase and mitochondrial dependent ROS generation [69,70]; superoxide generation by dysfunctional mitochondria in diabetes has been postulated as the initiating event in the development of diabetic complications [39]. It is possible that, while ASCs reduced inflammation, the anti-oxidative treatment of scaffolds with PGG prevented the expression of RAGE on injected and/or infiltrated cells, inhibiting the process of calcification.

Based on our results, we infer that the combination of autologous ASCs seeding and PGG pre-treatment of arterial elastin scaffolds could potentially lead to a functional tissue engineered construct able to achieve clinical translation of vascular tissue engineering in patients with diabetes.

In conclusion, autologous adipose stem cell seeding in arterial elastin scaffolds is effective in fighting diabetes-related complications seen in implanted grafts, due to the immunomodulatory and anti-inflammatory capabilities of stem cells. To prevent the calcification of elastin-based scaffolds implanted in diabetic conditions, the oxidative milieu needs to be reduced by elastin-binding antioxidants such as PGG.

### Acknowledgements

The authors also wish to thank the Godley Snell Research Center animal facility at Clemson University for outstanding help with the animal studies. Research reported in this paper was supported by an Institutional Development Award (IDeA) from the National Institute of General Medical Sciences of the National Institutes of Health under grant number P20GM103444-07 and in part by NHLBI of the National Institutes of Health under award number RO1HL093399, by the Harriet and Jerry Dempsey

Associate Professorship in Bioengineering Award and by a grant from the Romanian National Authority for Scientific Research, CNCS-UEFISCDI, project number PNII-ID-PCCE-2011-2-0036.

### Conflicts of Interest

The authors have no financial conflict of interest.

### Ethical Statement

This study was approved by the Animal Research Committee at Clemson University (AUP 2011-002).

All authors had participated actively and had a substantial contribution, as follows:

James P. Chow: scaffold preparation, immunohistochemistry and histology staining

Dan Simionescu: animal surgeries, IVIS imaging

Anna Lu Carter: stem cell isolation, seeding into scaffolds, histology quantification

Agnetta Simionescu: study coordination, writing the paper and final approval.

### REFERENCES

- Bierhaus A, Hofmann MA, Ziegler R, Nawroth PP. AGEs and their interaction with AGE-receptors in vascular disease and diabetes mellitus. I. The AGE concept. *Cardiovasc Res* 1998;37:586-600.
- Peterson LR, McKenzie CR, Schaffer JE. Diabetic cardiovascular disease: getting to the heart of the matter. *J Cardiovasc Transl Res* 2012;5:436-445.
- Fein FS. Diabetic cardiomyopathy. *Diabetes Care* 1990;13:1169-1179.
- Giacco F, Brownlee M. Oxidative stress and diabetic complications. *Circ Res* 2010;107:1058-1070.
- Roger VL, Go AS, Lloyd-Jones DM, Adams RJ, Berry JD, Brown TM, et al. Heart disease and stroke statistics--2011 update: a report from the American Heart Association. *Circulation* 2011;123:e18-e209.
- Whiting DR, Guariguata L, Weil C, Shaw J. IDF diabetes atlas: global estimates of the prevalence of diabetes for 2011 and 2030. *Diabetes Res Clin Pract* 2011;94:311-321.
- Bansal S, Siddarth M, Chawla D, Banerjee BD, Madhu SV, Tripathi AK. Advanced glycation end products enhance reactive oxygen and nitrogen species generation in neutrophils in vitro. *Mol Cell Biochem* 2012;361:289-296.
- Davi G, Falco A, Patrono C. Lipid peroxidation in diabetes mellitus. *Antioxid Redox Signal* 2005;7:256-268.
- Förstermann U. Oxidative stress in vascular disease: causes, defense mechanisms and potential therapies. *Nat Clin Pract Cardiovasc Med* 2008;5:338-349.
- Bierhaus A, Humpert PM, Morcos M, Wendt T, Chavakis T, Arnold B, et al. Understanding RAGE, the receptor for advanced glycation end products. *J Mol Med (Berl)* 2005;83:876-886.
- Del Turco S, Basta G. An update on advanced glycation endproducts and atherosclerosis. *Biofactors* 2012;38:266-274.
- Mezzetti A, Cipollone F, Cuccurullo F. Oxidative stress and cardiovascular complications in diabetes: isoprostanes as new markers on an old paradigm. *Cardiovasc Res* 2000;47:475-488.
- Forbes JM, Coughlan MT, Cooper ME. Oxidative stress as a major culprit in kidney disease in diabetes. *Diabetes* 2008;57:1446-1454.
- Tintut Y, Parhami F, Tsingotjidou A, Tetradis S, Territo M, Demer LL. 8-Isoprostaglandin E2 enhances receptor-activated NF-kappa B ligand (RANKL)-dependent osteoclastic potential of marrow hematopoietic precursors via the cAMP pathway. *J Biol Chem* 2002;277:14221-14226.
- Al-Aly Z. Arterial calcification: a tumor necrosis factor-alpha mediated vascular Wnt-opathy. *Transl Res* 2008;151:233-239.
- Qasim AN, Martin SS, Mehta NN, Wolfe ML, Park J, Schwartz S, et al. Lipoprotein(a) is strongly associated with coronary artery calcification in type-2 diabetic women. *Int J Cardiol* 2011;150:17-21.
- Alman AC, Maahs DM, Rewers MJ, Snell-Bergeon JK. Ideal cardiovascular health and the prevalence and progression of coronary artery calcification in adults with and without type 1 diabetes. *Diabetes Care* 2014;37:521-528.
- Mikos AG, Herring SW, Ochareon P, Elisseeff J, Lu HH, Kandel R, et al. Engineering complex tissues. *Tissue Eng* 2006;12:3307-3339.
- Bouten CV, Dankers PY, Driessen-Mol A, Pedron S, Brizard AM, Baaijens FP. Substrates for cardiovascular tissue engineering. *Adv Drug Deliv Rev* 2011;63:221-241.
- Chow JB, Simionescu DT, Warner H, Wang B, Patnaik SS, Liao J, et al. Mitigation of diabetes-related complications in implanted collagen and elastin scaffolds using matrix-binding polyphenol. *Biomaterials* 2013;34:685-695.
- Zhao J, Liu L, Wei J, Ma D, Geng W, Yan X, et al. A novel strategy to engineer small-diameter vascular grafts from marrow-derived mesenchymal stem cells. *Artif Organs* 2012;36:93-101.
- Kumar VA, Brewster LP, Caves JM, Chaikof EL. Tissue engineering of blood vessels: functional requirements, progress, and future challenges. *Cardiovasc Eng Technol* 2011;2:137-148.
- Harris LJ, Zhang P, Abdollahi H, Tarola NA, DiMatteo C, McIlhenny SE, et al. Availability of adipose-derived stem cells in patients undergoing vascular surgical procedures. *J Surg Res* 2010;163:e105-e112.
- Gimble J, Guilak F. Adipose-derived adult stem cells: isolation, characterization, and differentiation potential. *Cytotherapy* 2003;5:362-369.
- Gimble JM, Katz AJ, Bunnell BA. Adipose-derived stem cells for regenerative medicine. *Circ Res* 2007;100:1249-1260.
- Kronsteiner B, Wolbank S, Peterbauer A, Hackl C, Redl H, van Griensven M, et al. Human mesenchymal stem cells from adipose tissue and amnion influence T-cells depending on stimulation method and presence of other immune cells. *Stem Cells Dev* 2011;20:2115-2126.
- DelaRosa O, Lombardo E, Beraza A, Mancheño-Corvo P, Ramirez C, Menta R, et al. Requirement of IFN-gamma-mediated indoleamine 2,3-dioxygenase expression in the modulation of lymphocyte proliferation by human adipose-derived stem cells. *Tissue Eng Part A* 2009;15:2795-2806.
- Gonzalez-Rey E, Gonzalez MA, Varela N, O'Valle F, Hernandez-Cortes P, Rico L, et al. Human adipose-derived mesenchymal stem cells reduce inflammatory and T cell responses and induce regulatory T cells in vitro in rheumatoid arthritis. *Ann Rheum Dis* 2010;69:241-248.
- Rabbah JB, Saikrishnan N, Yoganathan AP. A novel left heart simulator for the multi-modality characterization of native mitral valve geometry and fluid mechanics. *Ann Biomed Eng* 2013;41:305-315.
- Anderson P, Souza-Moreira L, Morell M, Caro M, O'Valle F, Gonzalez-Rey E, et al. Adipose-derived mesenchymal stromal cells induce immunomodulatory macrophages which protect from experimental colitis and sepsis. *Gut* 2013;62:1131-1141.
- Waterman RS, Tomchuck SL, Henkle SL, Betancourt AM. A new mesenchymal stem cell (MSC) paradigm: polarization into a pro-inflammatory MSC1 or an immunosuppressive MSC2 phenotype. *PLoS One* 2010;5:e10088.
- Ebrahimi B, Eirin A, Li Z, Zhu XY, Zhang X, Lerman A, et al. Mesenchymal stem cells improve medullary inflammation and fibrosis after revascularization of swine atherosclerotic renal artery stenosis. *PLoS One* 2013;8:e67474.
- Tidball JG, Vallalta SA. Regulatory interactions between muscle and the immune system during muscle regeneration. *Am J Physiol Regul Integr Comp Physiol* 2010;298:R1173-R1187.

34. Badylak SF, Valentin JE, Ravindra AK, McCabe GP, Stewart-Akers AM. Macrophage phenotype as a determinant of biologic scaffold remodeling. *Tissue Eng Part A* 2008;14:1835-1842.
35. Zuk PA, Zhu M, Mizuno H, Huang J, Futrell JW, Katz AJ, et al. Multilineage cells from human adipose tissue: implications for cell-based therapies. *Tissue Eng* 2001;7:211-228.
36. Tuominen VJ, Ruotoistenmäki S, Viitanen A, Jumppanen M, Isola J. ImmunoRatio: a publicly available web application for quantitative image analysis of estrogen receptor (ER), progesterone receptor (PR), and Ki-67. *Breast Cancer Res* 2010;12:R56.
37. Brown BN, Ratner BD, Goodman SB, Amar S, Badylak SF. Macrophage polarization: an opportunity for improved outcomes in biomaterials and regenerative medicine. *Biomaterials* 2012;33:3792-3802.
38. Stöhr R, Federici M. Insulin resistance and atherosclerosis: convergence between metabolic pathways and inflammatory nodes. *Biochem J* 2013; 454:1-11.
39. Johansen JS, Harris AK, Rychly DJ, Ergul A. Oxidative stress and the use of antioxidants in diabetes: linking basic science to clinical practice. *Cardiovasc Diabetol* 2005;4:5.
40. Tollervy JR, Lunyak VV. Adult stem cells: simply a tool for regenerative medicine or an additional piece in the puzzle of human aging? *Cell Cycle* 2011;10:4173-4176.
41. Rehman J, Traktuev D, Li J, Merfeld-Claus S, Temm-Grove CJ, Bovenkerk JE, et al. Secretion of angiogenic and antiapoptotic factors by human adipose stromal cells. *Circulation* 2004;109:1292-1298.
42. Miranville A, Heeschen C, Sengenès C, Curat CA, Busse R, Bouloumié A. Improvement of postnatal neovascularization by human adipose tissue-derived stem cells. *Circulation* 2004;110:349-355.
43. Gimble JM, Guilak F, Bunnell BA. Clinical and preclinical translation of cell-based therapies using adipose tissue-derived cells. *Stem Cell Res Ther* 2010;1:19.
44. Yañez R, Oviedo A, Aldea M, Bueren JA, Lamana ML. Prostaglandin E2 plays a key role in the immunosuppressive properties of adipose and bone marrow tissue-derived mesenchymal stromal cells. *Exp Cell Res* 2010;316:3109-3123.
45. Jacobs E, Fuchte K, Bredt W. Amino acid sequence and antigenicity of the amino-terminus of the 168 kDa adherence protein of *Mycoplasma pneumoniae*. *J Gen Microbiol* 1987;133:2233-2236.
46. Duca L, Floquet N, Alix AJ, Haye B, Debelle L. Elastin as a matrikine. *Crit Rev Oncol Hematol* 2004;49:235-244.
47. Hinek A, Rabinovitch M. 67-kD elastin-binding protein is a protective "companion" of extracellular insoluble elastin and intracellular tropoelastin. *J Cell Biol* 1994;126:563-574.
48. Schulte JB, Simionescu A, Simionescu DT. The acellular myocardial flap: a novel extracellular matrix scaffold enriched with patent microvascular networks and biocompatible cell niches. *Tissue Eng Part C Methods* 2013; 19:518-530.
49. Barnes CA, Brison J, Michel R, Brown BN, Castner DG, Badylak SF, et al. The surface molecular functionality of decellularized extracellular matrices. *Biomaterials* 2011;32:137-143.
50. Belkin AM, Stepp MA. Integrins as receptors for laminins. *Microsc Res Tech* 2000;51:280-301.
51. Lanasa SM, Bryant SJ. Influence of ECM proteins and their analogs on cells cultured on 2-D hydrogels for cardiac muscle tissue engineering. *Acta Biomater* 2009;5:2929-2938.
52. Taki K, Takayama F, Tsuruta Y, Niwa T. Oxidative stress, advanced glycation end product, and coronary artery calcification in hemodialysis patients. *Kidney Int* 2006;70:218-224.
53. Chen NX, Moe SM. Arterial calcification in diabetes. *Curr Diab Rep* 2003; 3:28-32.
54. Lehto S, Niskanen L, Suhonen M, Rönnemaa T, Laakso M. Medial artery calcification. A neglected harbinger of cardiovascular complications in non-insulin-dependent diabetes mellitus. *Arterioscler Thromb Vasc Biol* 1996;16:978-983.
55. Moe SM, O'Neill KD, Duan D, Ahmed S, Chen NX, Leapman SB, et al. Medial artery calcification in ESRD patients is associated with deposition of bone matrix proteins. *Kidney Int* 2002;61:638-647.
56. Sakata N, Noma A, Yamamoto Y, Okamoto K, Meng J, Takebayashi S, et al. Modification of elastin by pentosidine is associated with the calcification of aortic media in patients with end-stage renal disease. *Nephrol Dial Transplant* 2003;18:1601-1619.
57. Anastasiadis K, Moschos G. Diabetes mellitus and coronary revascularization procedures. *Int J Cardiol* 2007;119:10-14.
58. Isenburg JC, Karamchandani NV, Simionescu DT, Vyavahare NR. Structural requirements for stabilization of vascular elastin by polyphenolic tannins. *Biomaterials* 2006;27:3645-3651.
59. Chuang TH, Stabler C, Simionescu A, Simionescu DT. Polyphenol-stabilized tubular elastin scaffolds for tissue engineered vascular grafts. *Tissue Eng Part A* 2009;15:2837-2851.
60. Yamauchi H, Motomura N, Chung UI, Sata M, Takai D, Saito A, et al. Growth-associated hyperphosphatemia in young recipients accelerates aortic allograft calcification in a rat model. *J Thorac Cardiovasc Surg* 2013; 145:522-530.
61. Simionescu A, Philips K, Vyavahare N. Elastin-derived peptides and TGF-beta1 induce osteogenic responses in smooth muscle cells. *Biochem Biophys Res Commun* 2005;334:524-532.
62. Simionescu A, Simionescu DT, Vyavahare NR. Osteogenic responses in fibroblasts activated by elastin degradation products and transforming growth factor-beta1: role of myofibroblasts in vascular calcification. *Am J Pathol* 2007;171:116-123.
63. Takemoto M, Yokote K, Yamazaki M, Ridall AL, Butler WT, Matsumoto T, et al. Enhanced expression of osteopontin by high glucose. Involvement of osteopontin in diabetic macroangiopathy. *Ann N Y Acad Sci* 2000;902:357-363.
64. Sodhi CP, Phadke SA, Batlle D, Sahai A. Hypoxia stimulates osteopontin expression and proliferation of cultured vascular smooth muscle cells: potentiation by high glucose. *Diabetes* 2001;50:1482-1490.
65. Choi ST, Kim JH, Kang EJ, Lee SW, Park MC, Park YB, et al. Osteopontin might be involved in bone remodelling rather than in inflammation in ankylosing spondylitis. *Rheumatology (Oxford)* 2008;47:1775-1779.
66. Anderson JM, Rodriguez A, Chang DT. Foreign body reaction to biomaterials. *Semin Immunol* 2008;20:86-100.
67. Higai K, Shimamura A, Matsumoto K. Amadori-modified glycated albumin predominantly induces E-selectin expression on human umbilical vein endothelial cells through NADPH oxidase activation. *Clin Chim Acta* 2006;367:137-143.
68. Zhang J, Li L, Kim SH, Hagerman AE, Lü J. Anti-cancer, anti-diabetic and other pharmacologic and biological activities of penta-galloyl-glucose. *Pharm Res* 2009;26:2066-2080.
69. Wautier MP, Chappay O, Corda S, Stern DM, Schmidt AM, Wautier JL. Activation of NADPH oxidase by AGE links oxidant stress to altered gene expression via RAGE. *Am J Physiol Endocrinol Metab* 2001;280: E685-E694.
70. Thallas-Bonke V, Thorpe SR, Coughlan MT, Fukami K, Yap FY, Sourris KC, et al. Inhibition of NADPH oxidase prevents advanced glycation end product-mediated damage in diabetic nephropathy through a protein kinase C-alpha-dependent pathway. *Diabetes* 2008;57:460-469.